

Regulation of Epidermal Tight-Junctions (TJ) during Infection with Exfoliative Toxin-Negative *Staphylococcus* Strains

Ulrich Ohnemus¹, Klaas Kohrmeyer¹, Pia Houdek¹, Holger Rohde², Ewa Wladykowski¹, Sabine Vidal¹, Matthias A. Horstkotte², Martin Aepfelbacher², Nina Kirschner¹, Martin J. Behne¹, Ingrid Moll¹ and Johanna M. Brandner¹

Tight Junction (TJ) proteins have been shown to exert a barrier function within the skin. Here, we study the fate of TJ proteins during the challenge of the skin by bacterial colonization and infection. We investigated the influence of various exfoliative toxin-negative *Staphylococcus* strains on TJ, adherens junction (AJ), desmosomal proteins, and actin in a human keratinocyte infection culture and in a porcine skin infection model. We found that the pathogen *Staphylococcus aureus* downregulates TJ and subsequently AJ and desmosomal proteins, including atypical protein kinase C, an essential player in TJ formation, at the cell-cell borders of keratinocytes in a time and concentration dependent manner. Little changes in protein and RNA levels were seen, indicating redistribution of proteins. In cultured keratinocytes, a reduction of transepithelial resistance was observed. *Staphylococcus epidermidis* shows only minor effects. All strains induced enhanced expression of occludin and ZO-1 at the beginning of colonization/infection. Thus, we demonstrate that TJ are likely to be involved in skin infection of exfoliative toxin-negative *S. aureus*. As we did not find a change in actin, and as changes of TJ preceded alterations of AJs and desmosomes, we suggest that *S. aureus* targets TJ.

Journal of Investigative Dermatology (2008) **128**, 906–916; doi:10.1038/sj.jid.5701070; published online 4 October 2007

INTRODUCTION

Tight Junctions (TJs) represent important intercellular junctions that are able to control paracellular diffusion of water, solutes, and pathogens (barrier function), and establish a “fence” between apical and basolateral domains of the plasma membrane which leads to the establishment and maintenance of cell polarity (for reviews see Tsukita and Furuse, 2002; Matter and Balda, 2003a; Schneeberger and Lynch, 2004; Furuse and Tsukita, 2006; Mertens *et al.*, 2006).

TJ are composed of transmembrane proteins, that is, members of the large claudin (Cldn) family, occludin, and members of the junctional adhesion molecule (JAM) family, binding to cytoplasmic proteins, so-called TJ-plaque proteins, including ZO-1-3, MUPP-1, and cingulin. There exist

structural as well as functional linkages between TJ and the actin filament cytoskeleton via various proteins (for review see Schneeberger and Lynch, 2004).

The existence of TJ in mammalian epidermis and their implication on epidermal barrier function has been shown only recently (Pummi *et al.*, 2001; Brandner *et al.*, 2002; Furuse *et al.*, 2002; Langbein *et al.*, 2002; Leyvraz *et al.*, 2005; Tunggal *et al.*, 2005; Brandner *et al.*, 2006). Typical TJ structures (“kissing points”) are restricted to the stratum granulosum, whereas TJ protein localization pattern in the epidermis is more complex; some TJ proteins are located in all viable layers (eg, Cldn-1, Cldn-7, MUPP-1, and JAM-A), while others are restricted to the stratum granulosum (eg, occludin) or are found in the upper layers of the epidermis (eg, ZO-1 and Cldn-4) (Brandner *et al.*, 2002, 2006). Several knockout mouse models which are directly (Cldn-1), or indirectly (due to the knock out of E-Cadherin and CAP1/Prss8, respectively), deficient for TJ proteins in the epidermis, as well as Cldn-6-overexpressing mice, are characterized by leaky TJ and die soon after birth due to a tremendous transepidermal water loss (Furuse *et al.*, 2002; Turksen and Troy, 2002; Leyvraz *et al.*, 2005; Tunggal *et al.*, 2005).

The skin displays an extensive interface between the individual and the surrounding environment. By an area of about 1.5–2.0 m² it constitutes a major target of microbial assaults. For manifestation of an infection, bacteria have to conquer the outside-in barrier of the skin. They have to invade the skin

¹Department of Dermatology and Venerology, University Hospital Hamburg-Eppendorf, Hamburg, Germany and ²Department of Medical Microbiology, Virology and Hygiene, University Hospital Hamburg-Eppendorf, Hamburg, Germany

Correspondence: Dr Johanna M. Brandner, Department of Dermatology and Venerology, University Hospital Hamburg-Eppendorf, University of Hamburg, Martinistrasse 52, D-20246 Hamburg, Germany.
E-mail: brandner@uke.uni-hamburg.de

Abbreviations: AJ, adherens junction; aPKC, atypical protein kinase C; ETA, exfoliate toxin A; ETB, exfoliate toxin B; JAM, junctional adhesion molecule; PKC, protein kinase C; TBST, tris buffered saline + triton; TER, transepithelial resistance; TJ, Tight Junction

Received 11 December 2006; revised 3 July 2007; accepted 8 July 2007; published online 4 October 2007

by traversing the stratum corneum and the living cell layers of the epidermis by a paracellular or transcellular pathway. Cell-cell junctions that have to be contacted during paracellular invasion comprise TJ, adherens junction (AJ), and desmosomes.

Skin infections with *Staphylococcus aureus* (*S. aureus*) are well-established causes of morbidity and mortality (Travers *et al.*, 2001). Infections by these bacteria not only directly cause ailments like abscess formation, impetigo contagiosa, and ecthymata (Murakawa, 2004; Iwatsuki *et al.*, 2006), but are triggers in worsening inflammatory skin diseases like atopic dermatitis (Leung *et al.*, 1998; Breuer *et al.*, 2005). The ability of *S. aureus* to cause disease in humans can be attributed to the expression of a wide array of factors promoting bacterial adhesion to eukaryotic cells and extracellular matrix molecules on one hand, and on the other hand to the production of toxins which directly cause tissue damage (Iwatsuki *et al.*, 2006). In the context of cutaneous infections the exfoliative toxins have gained major interest, and it was demonstrated that these toxins may induce desmosome damage by cleaving desmoglein 1, leading to *Staphylococcus* scalded skin syndrome. Effects on TJ or AJ have not been described (Amagai *et al.*, 2000, 2002; Fudaba *et al.*, 2005).

Importantly, the expression of exfoliative toxins is not a *condition sine qua non* for *S. aureus* to cause infections of the skin. However, not much is known about mechanisms of infections of exfoliative toxin-negative strains. In addition there are no data available stating the regulation of TJ during *Staphylococcus* skin infections. As we learned from simple epithelia, TJ can be involved in a variety of host-pathogen interactions (for review see Fasano, 2001, 2002; Laukoetter *et al.*, 2006).

To elucidate the fate of TJ in bacterial skin infection, we investigated TJ proteins during infection with various strains of *S. aureus* and the non-pathogenic commensal *Staphylococcus epidermidis*. We used the human keratinocyte cell line HaCat and a porcine *ex vivo* skin infection model. In addition, we investigated infected human skin diagnosed with impetigo contagiosa. For evaluation of the functional capability of the TJ we investigated transepithelial electrical resistance of HaCaT cells infected with *S. aureus* and *S. epidermidis*. Since TJ are dynamically interconnected with the actin cytoskeleton, AJ, and desmosomes, it was of interest to elucidate whether marker proteins of these structures are concomitantly affected.

RESULTS

Expression and localization of TJ, AJ, and desmosomal proteins, as well as actin in HaCaT cells after *Staphylococcus* infection with *S. aureus* clinical isolate, ATCC 29213 and *S. epidermidis* 1457

To investigate whether there are differences within the localization patterns of intercellular junction proteins after infections with diverse *Staphylococcus* strains (*S. aureus* clinical isolate (ci), ATCC 29213, and *S. epidermidis* 1457, concentrations of 10^{4-6} bacteria per ml) and the non-infected control groups, we studied the localization of: TJ proteins Cldn-1, Cldn-4, occludin, and ZO-1, AJ proteins E-Cadherin and β -Catenin, and desmosomal proteins desmoplakin I + II,

3 and 5 hours after initiation of infection. As a key player in TJ formation, localization of atypical protein kinase C (PKC) was determined as well. To evaluate changes of the cytoskeleton we analyzed actin stained with rhodamine-phalloidin.

S. aureus (clinical isolate and ATCC 29213) produced significant changes of intensity of immunostainings at the cell-cell borders in a time- and dose-dependent manner. There were no marked changes 3 hours following infection with all *Staphylococcus* strains independent of concentration (10^{4-6} per ml). However, we saw a slight (10^4 bacteria per ml) and even a marked decrease (10^5 bacteria per ml) of the TJ proteins Cldn-1 (Figure 1a and b; all data shown for *S. aureus* ATCC), Cldn-4 (data not shown), occludin (Figure 1d and e), and ZO-1 (Figure 1g and h; Figure S1a, b, g, h) at the cell-cell borders 5 hours after infection with *S. aureus*. With concentrations of 10^6 *S. aureus* cells per ml, the downregulation of the proteins was even more pronounced (data not shown). Interestingly, we observed an almost complete loss of junctional staining for atypical PKC with *S. aureus* 10^5 /ml 5 hours following infection (Figure 1j and k; Figure S1j, k, p, q). AJ proteins E-Cadherin (Figure 1m and n; Figure S1d, e, g, h, m, n, p, q) and β -Catenin (data not shown), as well as desmosomal proteins desmoplakin I + II (Figure 1p and q) were also downregulated, but to a lesser extent. The phalloidin staining pattern of actin remained unaffected after staphylococcal infection (Figure 1s and t).

S. epidermidis infection induced a slight loss of ZO-1 immunoreactivity in a concentration of 10^{5-6} /ml 5 hours following infection, but did not affect any of the other antibodies' immunoreactivity within the HaCat cell culture irrespective of time and concentration (Figure 1; Figure S1). We next evaluated protein levels by Western blot analysis, and we found no differences in the total amount of Cldn-1, Cldn-4, Cldn-7, JAM-A, E-Cadherin, and β -Catenin between control and infected cells (Figure 2). There was a slight decrease of the amount of ZO-1 with 10^5 /ml *S. aureus*, and for ZO-1, occludin, and atypical protein kinase C (aPKC) with 10^6 /ml *S. aureus*, 5 hours after the induction of infection (Figure 2). Using real-time PCR we noticed a slight upregulation of RNA levels for the molecules investigated (Cldn-4, Occl, and ZO-1) 3 hours after infection with *S. aureus*, for occludin also with *S. epidermidis* 1457 (Table 1). In summary, level of immunofluorescence staining at the cell-cell borders of the TJ proteins is considerably altered, whereas only little changes in protein and RNA levels are seen.

Decrease of transepithelial resistance after *S. aureus* infection

To show the functional significance of our findings, we performed transepithelial resistance (TER) experiments with HaCaT cells infected with *S. aureus* and *S. epidermidis*. As demonstrated in Figure 3, there was a significant decrease of TER in HaCaT cell monolayers infected with *S. aureus* compared with the control group, and the cells infected with *S. epidermidis*. After 3 hours already, a decrease of TER could be observed after infection with *S. aureus*, this decrease became steadily more pronounced within a time course of 10 hours. Interestingly, compared with the control group, infection of the cell monolayers with *S. epidermidis* induced

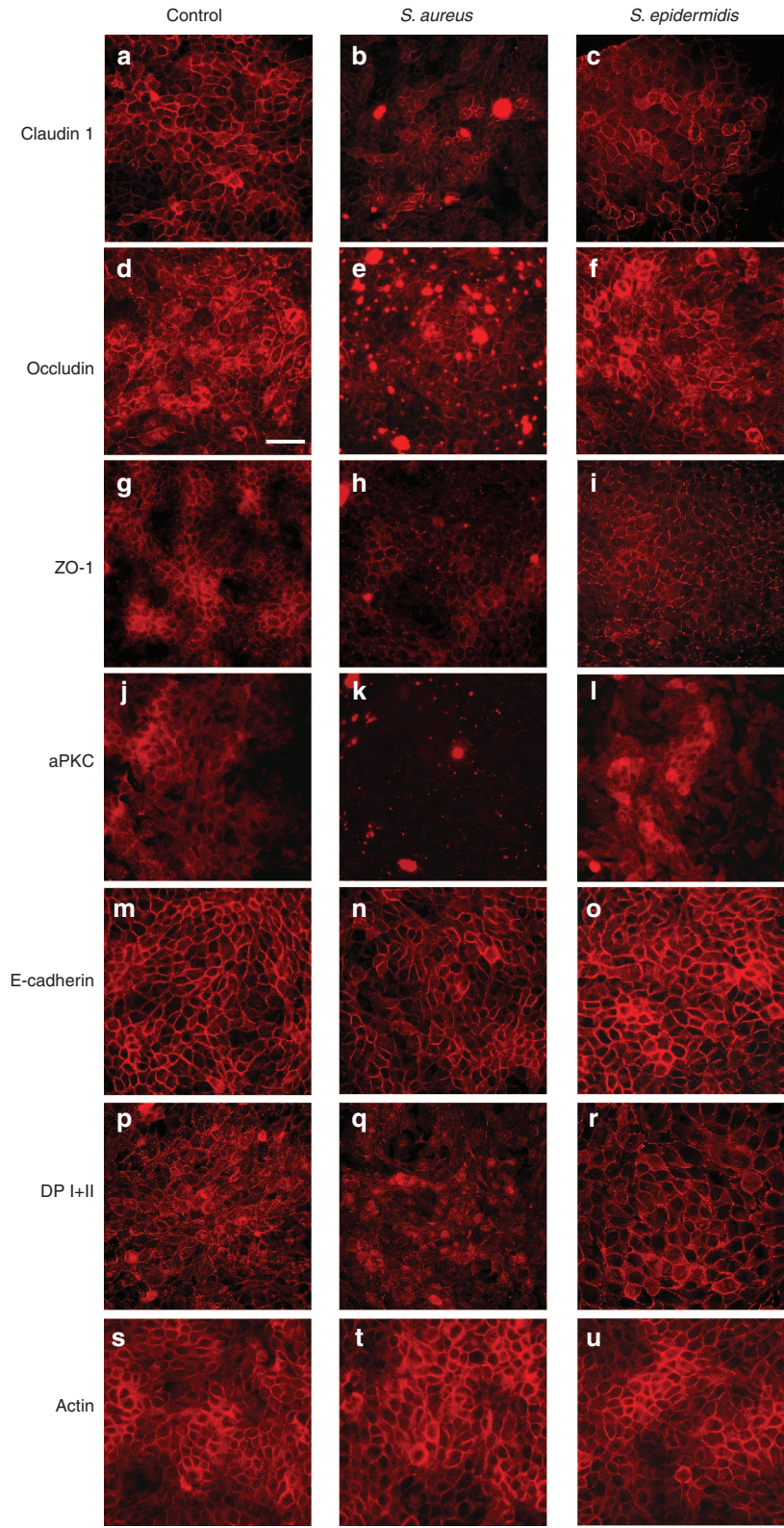


Figure 1. Immunolocalization of TJ, AJ, desmosomal proteins, and actin in uninfected HaCaT cells and after *Staphylococcus* infection with *S. aureus* ATCC 29213 and *S. epidermidis* 1457. Immunofluorescence microscopy showing the localization of (a-c) Cldn-1, (d-f) occludin, (g-i) ZO-1, (j-l) aPKC, (m-o) E-Cadherin, (p-r) desmoplakin I+II (DP), and (s-u) actin 5 hours after infection with 10^5 /ml *S. aureus* ATCC 29213 (b, e, h, k, n, q, t) and 10^5 /ml *S. epidermidis* 1457 (c, f, i, l, o, r, u). (a, d, g, j, m, p, s) Control cultures without infection. Note the downregulation of immunoreactivity at the cell-cell borders by *S. aureus* 29213. The accessory red dots visible in section (b, e, h, k, q) most probably represent IgG bound to the *S. aureus* surface via Protein A, reflecting a pathogenicity factor of *S. aureus*. Bar = 50 μ m.

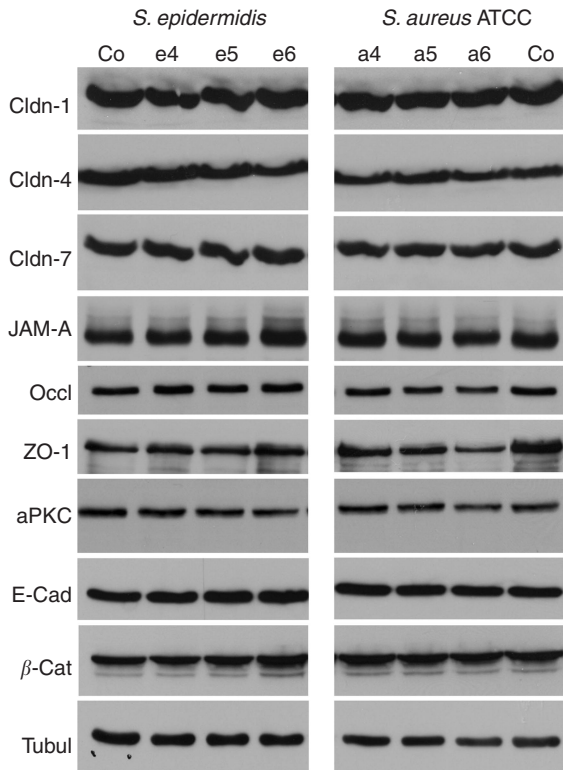


Figure 2. Protein expression of TJ and AJ proteins 5 hours after bacterial infection. HaCaT cells were infected with different concentrations of *S. epidermidis* 1457 (left side: Co: control cells, no infection; e4: infection with 10^4 bacterial cells per ml; e5: 10^5 cells/ml; e6: 10^6 cells/ml) and *S. aureus* ATCC 29213 (right side: a4: infection with 10^4 bacterial cells per ml; a5: 10^5 cells/ml; a6: 10^6 cells/ml; Co: control cells, no infection) for 5 hours and subsequently lysed. Equal amounts of proteins were separated by SDS-PAGE and immunoblotted with antibodies specific for the proteins indicated. α -Tubulin was used as gel loading control.

Table 1. Transcriptional differences between infected and non-infected keratinocytes¹

	<i>S. aureus</i> ATCC 29213			<i>S. epidermidis</i> 1457		
	Claudin-4	Occludin	ZO-1	Claudin-4	Occludin	ZO-1
3 h	3	2.6	1.8	1.5	1.4	1.3
5 h	1.9	1.6	1.5	1.3	1.5	1.3

¹The differences of transcription (*n*-fold) between infected and non-infected cells were calculated by the $2^{-\Delta\Delta C_t}$ method. Values represent the means of results from five (3 hours) and three (5 hours) independent experiments. Significant differences are set in bold.

an initial increase of TER within the first 6 hours of infection. This increase was followed by a slight decrease of TER 9 and 10 hours following infection with *S. epidermidis*.

Localization of TJ, AJ, and desmosomal proteins as well as actin in porcine skin, 24 hours following *Staphylococcus* infection with *S. aureus* clinical isolate, ATCC 29213 and *S. epidermidis*

To examine whether the changes in the distribution of junctional proteins observed in the two dimensional cell-culture

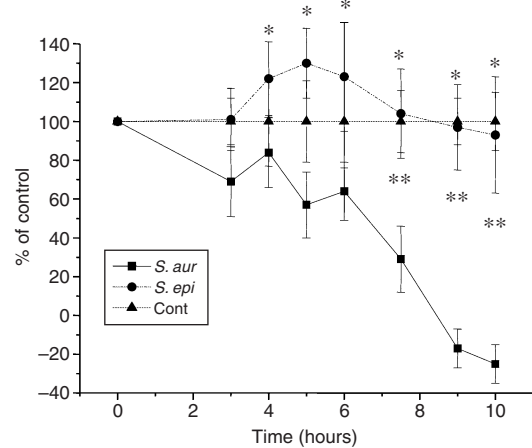


Figure 3. TER of HaCaT cells after infection with *S. aureus* and *S. epidermidis*. TER of HaCaT cell monolayers after infection with *S. aureus* ATCC 29213 (squares) and *S. epidermidis* 1457 (circles), normalized to uninfected control cells (triangles). Given are the percentages in correlation to the control, which was standardized as 100%. Values represent mean \pm SEM ($n=6$). Differences between control cells and cells infected with *S. aureus* are statistically significant ($P \leq 0.05$) at >7.5 hours (double asterisks), those between cells infected with *S. epidermidis* and *S. aureus* at >4 hours (single asterisk) after infection.

model were also visible in a more physiological setting (intact epidermis), we established an *ex vivo* infection model of porcine skin (see Materials and Methods).

We assessed the effects of *S. aureus* clinical isolate and ATCC 29213 in a 24 hours infection series. The 24-hour period was chosen because a slower induction of inter-cellular junction alterations was expected in the three-dimensional model compared with the HaCaT cells due to the stratum corneum barrier function. Classified by semi-quantitative evaluation of the stainings, results were divided into normal immunoreactivity, enhanced immunoreactivity, reduced immunoreactivity, and loss of immunoreactivity, 24 hours following staphylococcal infections. In general, throughout all infection models investigated, there were areas with changes of immunofluorescence staining neighboring areas with unaffected staining presumably due to intensity of bacterial infection. Cldn-1 immunoreactivity was significantly downregulated by both *S. aureus* strains (see Figure 4a and b for ATCC; for clinical isolate not shown). A similar tendency could be observed for ZO-1 (Figure 4d and e), occludin (data not shown), E-Cadherin (Figure 4g and h), β -Catenin (data not shown), and to a lesser extent desmoplakin I+II (Figure 4j and k). No changes were seen in the staining pattern of the actin cytoskeleton (Figure 4m and n). Unfortunately, antibodies to aPKC were not reactive on porcine skin. Most skin models infected with *S. epidermidis* 1457 did not show a loss of staining of junctional proteins or actin (Figure 4c, f, i, l, o). In about 20% a loss of ZO-1 staining, and in about 10% a loss of Cldn-1 and occludin staining was observed (data not shown). E-Cadherin, β -Catenin, and desmoplakin I+II remained completely unaffected.

To ensure that the above observed effects were not the result of impaired viability of the infection models, we investigated

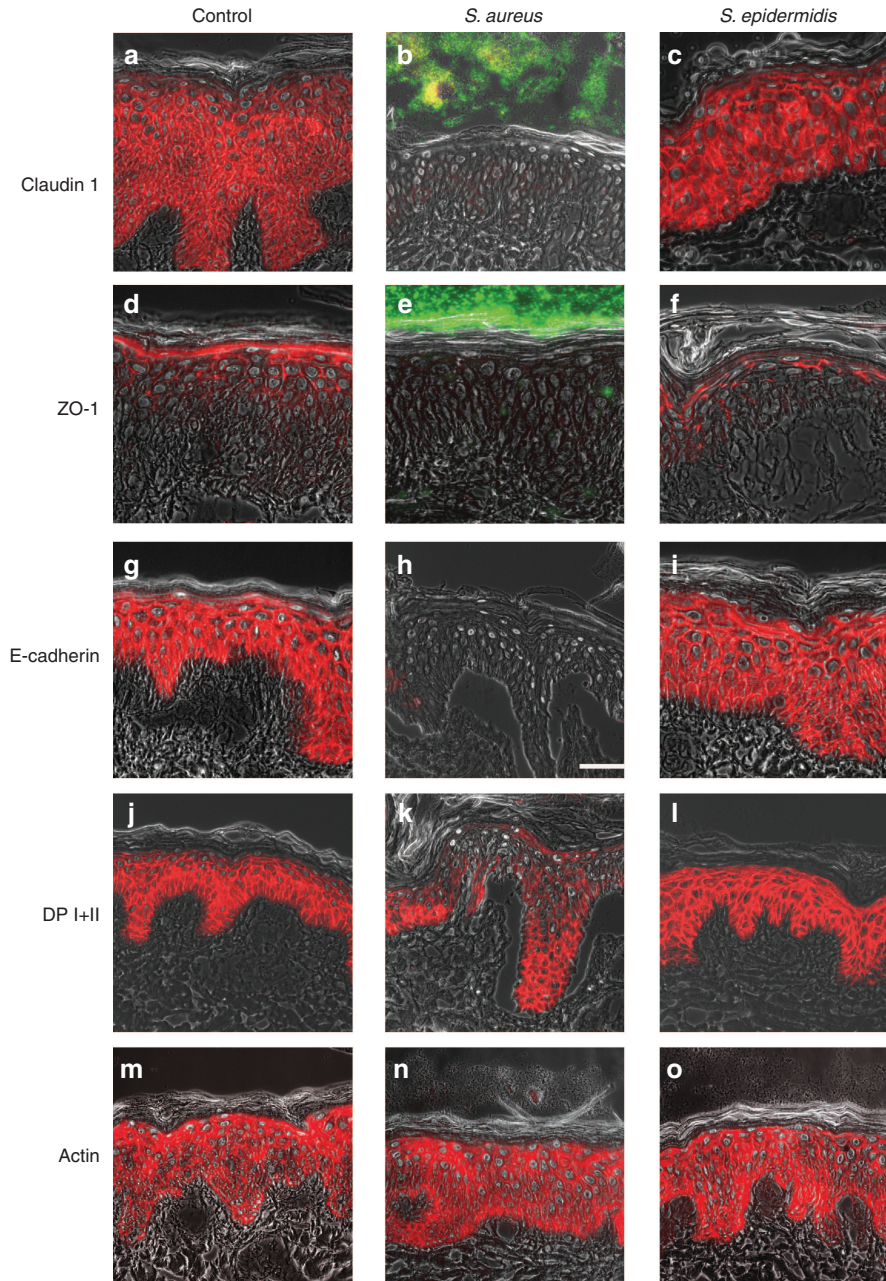


Figure 4. Localization of TJ, AJ, desmosomal proteins, and actin in porcine skin infection models 24 hours following infection with *S. aureus* ATCC 29213 and *S. epidermidis* 1457. Immunofluorescence microscopy of frozen sections of the porcine skin infection model showing the immunolocalization of (a-c) Cldn-1, (d-f) ZO-1, (g-i) E-Cadherin, (j-l) desmoplakin I + II (DP), and (m-o) actin 24 hours after staphylococcal infection. (a, d, g, j, m) Control without infection; (b, e, h, k, n) *S. aureus*; (c, f, i, l, o) *S. epidermidis*; (red) intercellular junction proteins, (green) *S. aureus* Protein A. Protein A staining is only shown in b and e. Note the downregulation of immunoreactivity at the cell-cell borders by *S. aureus*. Bar = 50 μ m.

the amount of proliferative and apoptotic cells 24 hours after infection. The proliferation and apoptosis rates did not differ significantly between control and infected samples (Figure 5).

Localization of TJ, AJ, and desmosomal proteins in porcine skin 6 and 12 hours following *Staphylococcus* infection with *S. aureus* clinical isolate, ATCC 29213 and *S. epidermidis* 1457

To further evaluate the dynamics of intercellular junction protein localization changes, we checked immunoreactivity

of the TJ proteins ZO-1, Cldn-1, and occludin, AJ proteins E-Cadherin and β -Catenin, and desmosomal proteins desmoplakin I + II after periods of 6 and 12 hours following infection with *S. aureus* clinical isolate, ATCC 29213 and *S. epidermidis* 1457.

A widespread loss of staining was detected more than twice as much for ZO-1 (22% after 6 hours/100% after 12 hours) compared with Cldn-1 (11/50%) and occludin (10/50%) following 6 and 12 hours of infection with *S. aureus*

ATCC 29213. The same was found for *S. aureus* clinical isolate, but less accentuated (Figure S2a–c, f–h). The AJ proteins E-Cadherin (Figure S2d and i) and β -Catenin (not shown), as well as the desmosomal proteins desmoplakin I+II (Figure S2e and j) exerted no loss of staining at those time points. The same was true for all proteins in control models and models infected with *S. epidermidis* 1457 (Figure S2), except for occludin 12 hours after infection with this strain (Figure S2g).

TJ proteins Cldn-1 and ZO-1 showed in some models a reduction (no complete loss) of immunoreactivity within 6 and 12 hours following infection with both *S. aureus* strains (Figure S2a, c, f, h). To a lesser extent, a reduction of

immunoreactivity induced by *S. aureus* ATCC 29213 was also found for occludin (6 hours; Figure S2b) and E-Cadherin (12 hours; Figure S2i). ZO-1 also showed a reduced staining in 25% of models infected with *S. epidermidis* 1457 (Figure S2h).

In addition to the downregulation described above, skin models infected with *S. aureus* strains (ATCC 29213 and clinical isolate) concomitantly showed enhanced staining for occludin (Figure 6) and ZO-1 (data not shown) in neighboring areas. Also infection with *S. epidermidis* 1457 induced upregulation of occludin (Figure 6) and ZO-1 (data not shown) after 6, 12, and 24 hours.

Comparison of the effects of different *S. aureus* strains 24 hours after infection

It is well known that, dependent on the genetic background, *S. aureus* strains possess pathogenic potential in specific clinical settings. In order to delineate potential factors involved in the modifications of cell-cell junction proteins observed in this study, we assessed the effects of the different, well defined *S. aureus* strains RN 6390 and Newman in addition to *S. aureus* clinical isolate and ATCC 29213 in another 24 hours infection series. Figure S3 illustrates an overview of the different strains applied in these experiments. Of interest, *S. aureus* ATCC 29213, clinical isolate, and Newman induced more often loss of immunoreactivity in TJ and AJ proteins than RN 6390 (Figure S3a–d). On the other hand, neither *S. aureus* Newman nor RN 3690 induced loss of desmoplakin I+II (Figure S3e), demonstrating that different *S. aureus* strains exert strain-specific effects on intercellular structures. These differences might be attributed to the presence or absence of genes encoding extracellular

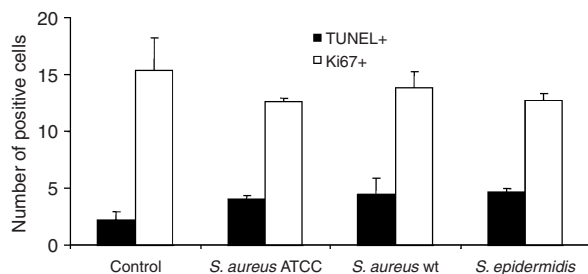


Figure 5. Proliferation and apoptosis within porcine skin infection models 24 hours following infection with *S. aureus* ATCC 29213, *S. aureus* clinical isolate, and *S. epidermidis* 1457. Quantitative analysis of TUNEL-positive cells shows a slight increase in *S. aureus*- and *S. epidermidis*-treated samples compared with the uninfected controls, whereas Ki67+ (proliferative) cells were decreased in the infection groups compared with uninfected control skin. The difference between the four groups ($n=5$ /group, count of three visual fields per individual skin sample) was not significant; (black) TUNEL+ and (white) Ki67+ cells. The graph shows mean values (\pm SEM).

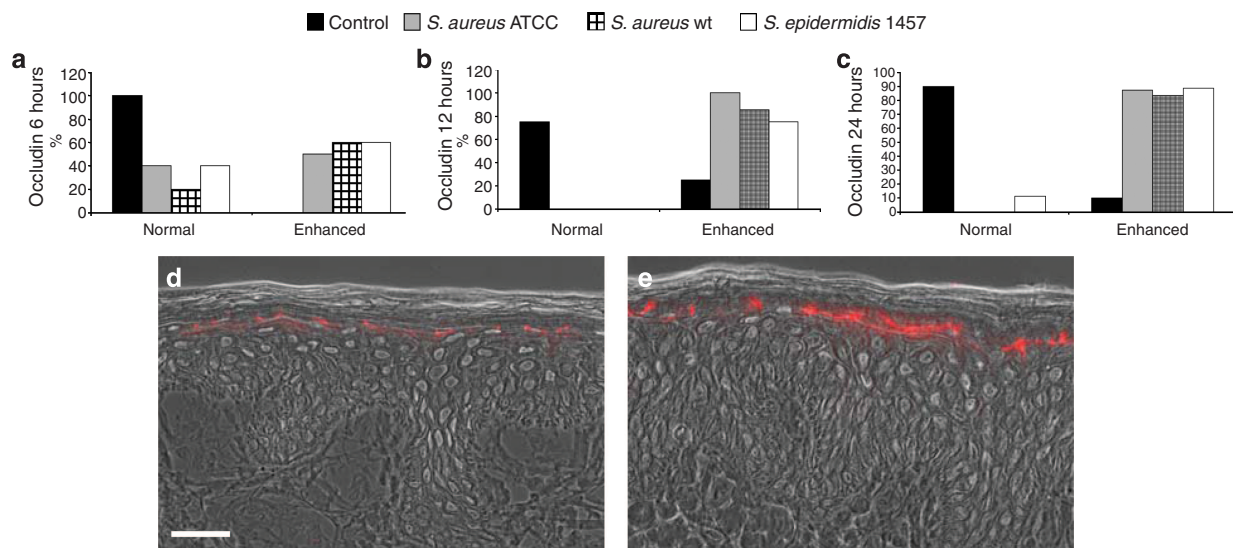


Figure 6. Immunoreactivity of TJ protein occludin in porcine skin infection models 6, 12, and 24 hours following *Staphylococcus* infection with *S. aureus* ATCC 29213, clinical isolate, and *S. epidermidis* 1457. The graphs reflect evaluations of immunoreactivity in frozen sections of the porcine infection model following (a) 6 hours, (b) 12 hours, and (c) 24 hours of *Staphylococcus* infection. As demonstrated by the photographs in (d) (control) and (e) (24 hours after infection with *S. epidermidis*), staining results were classified into “normal staining”, that is, as found in normal (porcine) skin (d) and enhanced staining (e). Black bars indicate uninfected control; gray: *S. aureus* ATCC 29213; black and white squares: *S. aureus* clinical isolate; and white: *S. epidermidis* 1457. Bar = 50 μ m.

matrix-binding proteins or toxins involved in the induction of epidermal lesions.

Cna and *bbp* (encoding a collagen- and a bone-sialo-protein-binding protein, respectively) were found in neither strain. *fnbA*, *clfA*, *spa*, *sdrD*, *map/eap*, and *sasG* were present in *S. aureus* Newman, ATCC 29213, and *S. aureus* RN 6390. In contrast, *S. aureus* clinical isolate lacked, apart from *cna* and *bbp*, also *sdrD* and *sasG* (Table S1). Regarding the distribution of exotoxins, *S. aureus* ATCC 29213 and clinical isolate both were negative for TSST-1, exfoliative toxin A/B, Panton-Valentine leukocidin, and leukozidin M. *S. aureus* ATCC 29213 was positive for leukozidin D and E. Both toxins were absent in *S. aureus* clinical isolate.

Immunolocalization of TJ proteins in infected human skin

Consistent with our results seen in porcine skin, we found a downregulation as well as a concomitant upregulation of ZO-1 (Figure 7b) and occludin (Figure 7d) at the cell-cell borders in infected human skin diagnosed with impetigo contagiosa. Also for Cldn-1 a slight downregulation was observed (Figure 7f). There was no change in staining patterns for E-Cadherin and desmoplakin (data not shown).

DISCUSSION

Having evaluated localization and expression of different TJ proteins in the human keratinocyte cell line HaCat and in

a porcine skin infection model after bacterial infection with different exfoliative toxin-negative *S. aureus* strains, our data show that TJ proteins Cldn-1, Cldn-4, ZO-1, and occludin are downregulated at the intercellular borders in a time and concentration dependant manner. This downregulation is accompanied by a loss of TER proving the functional significance of our observations. A downregulation of TJ proteins was also observed in infected human skin diagnosed with impetigo contagiosa. AJ proteins E-Cadherin and β -Catenin, as well as desmosomal proteins desmoplakin I + II were downregulated to a lesser extent. An almost complete loss was observed for atypical PKC. The phalloidin staining pattern of actin remained unaffected in both test models.

Only very restricted data is available concerning the fate of TJ proteins during bacterial skin infections. To our knowledge, the only report published shows a loss of ZO-1 at cell-cell junctions after infection with Group A streptococci of monolayers of cultured keratinocytes, but a correlation to epidermis is still missing (Cywes and Wessels, 2001). On the other hand, plenty of reports have shown that TJ are preferential sites to be attacked by invading pathogens in simple epithelia (for review see Fasano, 2001, 2002; Laukoetter *et al.*, 2006). Pathogens can influence TJ directly by cleavage or redistribution of TJ proteins, or indirectly by modifying the actin cytoskeleton and AJ, and by activation of cellular signal transduction pathways (Laukoetter *et al.*, 2006). All of these mechanism result in an opening of TJ and an increase of paracellular permeability.

The reduction or even loss of junctional staining occurred in a strictly time dependent manner. At first aPKC and ZO-1 disappeared (Figure 1; Figure S2), this was followed by Cldn-1 and occludin (Figure S2). Subsequently a loss of AJ proteins E-Cadherin and β -Catenin and finally of desmosomal proteins could be observed (Figure S2). The actin cytoskeleton, well known as a driving force for epithelial cell adhesion and AJ formation (Vasioukhin *et al.*, 2000), and connected to both AJ and TJ (Matter and Balda, 2003b), remained unchanged. As we did not find a change in actin cytoskeleton, and as changes in AJ and desmosomes were following the alterations of TJ, we suggest that host-pathogen interactions in exfoliative toxin-negative *S. aureus* skin infection are primarily directed to TJ.

Previously it was shown that the AJ protein E-Cadherin is not only necessary for AJ formation, but its adhesive activity is also crucial for the assembly of other junctional complexes such as TJ and desmosomes (eg, Lewis *et al.*, 1994; Tunggal *et al.*, 2005). During the formation of cell-cell junctions, Tiam-1-Rac signalling activates the Par3-Par6-aPKC complex, which is localized in primordial adhesions consisting of E-Cadherin and additional AJ, as well as TJ proteins. The activation results in a further recruitment of TJ proteins, the formation of separated TJ and AJ, and functionality of TJ (Schneeberger and Lynch, 2004; Mertens *et al.*, 2006). The effects observed in our study after infection with *S. aureus* might be explained by a partly inversion of this assembly process, starting with a loss of TJ proteins, initiated by aPKC and ZO-1, and ending with the loss of E-Cadherin. Interestingly, Cywes and Wessels (2001) showed that Group A

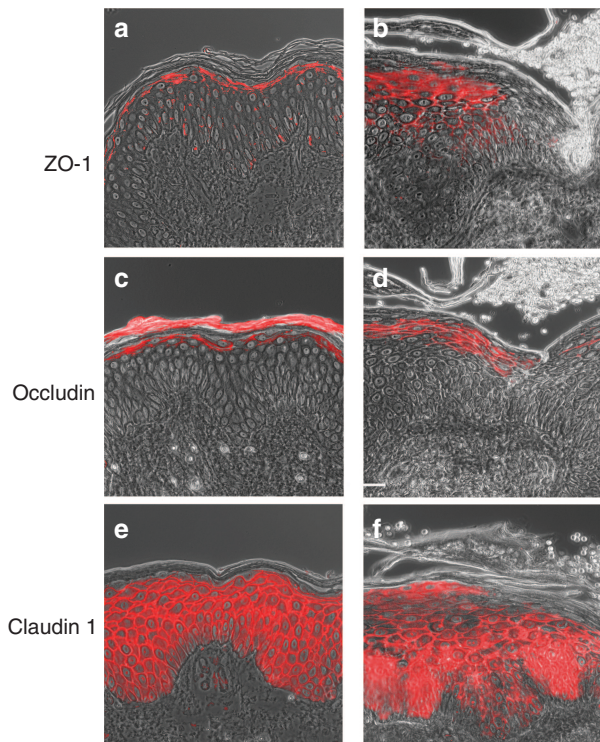


Figure 7. Immunoreactivity of TJ proteins in infected human skin. Immunofluorescence staining of (a, b) ZO-1, (c, d) occludin, and (e, f) Cldn-1 in normal human skin (a, c, e) and human skin diagnosed with impetigo contagiosa (b, d, f). Note the downregulation of ZO-1 and occludin in areas covered with bacteria and a concomitant upregulation in the neighboring areas. Bar = 50 μ m.

streptococci bind to CD44 in cultured keratinocytes, which results in a loss of E-Cadherin and ZO-1 at cell-cell junctions, a process which involves Rac1, ezrin, and tyrosin phosphorylation. Rac1 on the other hand is involved in Tiam signalling, which activates aPKC (Mertens *et al.*, 2006). Therefore, it will be interesting to investigate in future experiments whether upstream signals in staphylococcal infection also involve CD44.

On the protein level it can clearly be seen that the total amount of Claudins and JAM-A, as well as E-Cadherin and β -Catenin is not changed which hints for a redistribution instead of degradation of these proteins. A redistribution of TJ proteins after bacterial infection has been observed before in simple epithelia (eg, Muza-Moons *et al.*, 2004). On the other hand, a slight degradation of aPKC, occludin and ZO-1 can be observed. As this degradation is seen for aPKC and occludin only with 10^6 /ml bacteria while loss of junctional staining is already clearly seen with 10^5 /ml, the degradation might follow redistribution. The same applies to ZO-1, as a slight decrease of this protein can already be seen with 10^4 /ml bacteria, while a loss of protein amount is only seen with 10^5 /ml.

Infection of cells resulted in an early upregulation (3 hours) of Cldn-4, occludin, and ZO-1 on RNA level (Table 1). We investigated these molecules on the RNA level, as we learned that these proteins are upregulated in diseases with intrinsic impaired barrier function, for example, psoriasis (Pummi *et al.*, 2001; Yoshida *et al.*, 2001; Brandner *et al.*, 2006), and therefore might be altered by extrinsic barrier challenge, too. The upregulation of occludin and ZO-1 could also be confirmed in immunostaining of *ex vivo* infection models (enhancement of staining). Interestingly, this effect was not only detected with the pathogenic *S. aureus*, but also with the commensal, widely apathogenic *S. epidermidis*. In TER experiments we observed an increase of TER after infection with *S. epidermidis*. After infection with *S. aureus*, only a slight decrease of TER was seen at the beginning of infection, possibly reflecting a destruction of TJ at some areas and an improved barrier function in other areas of the cell monolayers. Later on, the destruction of TJ might be prevailing, therefore inducing a more pronounced loss of TER (>7.5 hours after infection). The upregulation of TJ proteins might be a kind of rescue mechanism after the contact of keratinocytes with bacteria, irrespective of their pathogenicity.

Using different *S. aureus* strains we could see comparable effects of *S. aureus* ATCC 29213, clinical isolate, and Newman, while *S. aureus* RN 6390 induced less alterations (Figure S3). One potential reason for the observed differences is the differential distribution of genes encoding colonization factors within the independent *S. aureus* strains. As *S. aureus* clinical isolate induced TJ alterations to the same degree as *S. aureus* ATCC 29213, we conclude from our results that at least SdrD and SasG, which are not expressed by *S. aureus* clinical isolate, but all the other strains, including RN 6390, are not by all means necessary for the induction of TJ damage by *S. aureus*. As TSST-1, exfoliative toxins A and B, Panton-Valentine leukozidin, leukozidin E, D, and M were negative in *S. aureus* clinical isolate, we can exclude that these factors

are basically necessary for the alterations observed. The exact underlying mechanisms will be subject of further studies. Nevertheless we cannot exclude that TJ might be involved in the pathomechanism of skin infection with exfoliative toxin-positive strains. However, it is unlikely that TJ are involved in blister formation induced by exfoliative toxin-positive or -negative strains because TJ are cell-cell junctions important for sealing cells to omit uncontrolled paracellular transport. They are not primarily involved in cell-cell adhesion, as for example, desmosomes, which have been shown to be cleaved by exfoliative toxin A (ETA) and exfoliative toxin B (ETB) (Amagai *et al.*, 2000, 2002; Fudaba *et al.*, 2005). Therefore, putative blister formation might be an event following the overcoming of TJ barrier with a consequent disruption of desmosomes.

The effects described in this paper are due to the application of bacteria to the apical part of porcine skin infection models and of HaCaT cell monolayers (upper chamber of the transwell filters in our TER experiments). However, we cannot exclude that bacteria or their toxins might also have had access to the basolateral part of the cells. Sonoda and co-workers have elegantly shown that incubation of cells with a C-terminal fragment of *Clostridium perfringens* enterotoxin only resulted in a loss of claudin 4 at the cell cell-borders and a decrease of TER when applied to the basolateral, but not to the apical compartment. This suggests that TJ work as the outside-in barrier to the C-terminal fragment of *C. perfringens* enterotoxin (Sonoda *et al.*, 1999). Whether similar or different mechanisms apply to *S. aureus* infection in skin still needs to be elucidated.

Our results clearly show that TJ proteins are dislocalized by epidermal invasion of bacteria. The response of TJ proteins on bacterial infection suggests that TJ might not only be involved in inside-out barrier function of the skin but also in outside-in barrier. However, the molecular mechanisms regarding how *S. aureus* regulates TJ and their contribution to outside-in barrier has to be elucidated in future experiments.

MATERIALS AND METHODS

Keratinocytes, tissues, and bacterial strains

Human cultured keratinocytes of line HaCaT were obtained from the laboratory of Professor Fusenig, Heidelberg, Germany (Boukamp *et al.*, 1988).

Human infected skin which was diagnosed as impetigo contagiosa was used after diagnostic procedures had been completed and in agreement with the local medical ethics committee (OB-14/04).

Porcine skin was obtained from a local slaughterhouse. All the pigs were of the same age and race.

The bacterial strains used in this study are summarized in Table S1. The clinical isolate was biochemically identified as *S. aureus* by using the ApiStaph gallery (BioMerieux, Marci l'Etoile, France).

Experiments were carried out with the institutional approval and in adherence to the Declaration of Helsinki Principles.

Antibodies, nuclear dyes, and primers

Antibodies specific for Cldn-1 (MH25), Cldn-4 (ZMD.306), Cldn-7 (ZMD.241), occludin (OC-3F10), and protein ZO-1 (Z-R1) were

purchased from Zymed Laboratories (San Francisco, CA). Antibodies specific for JAM-A (AF1103) were purchased from R&D systems (Minneapolis, MN), aPKC ζ (sc216) from Santa Cruz Biotechnology (Santa Cruz, CA), desmoplakin I and II (2.15/2.17/2.20) and E-Cadherin for human stainings (5H9) from Progen (Heidelberg, Germany), for β -Catenin (clone 14) from Transduction Laboratories (Lexington, KY), for E-Cadherin for porcine stainings (M3612) and Ki-67 (MIB-1) from Dako (Hamburg, Germany), for Protein-A (SPA-27) from Sigma (Taufkirchen, Germany), and α -Tubulin (CP06) from Calbiochem (Darmstadt, Germany). Texas Red-labeled phalloidin (T7471) for actin staining was from MoBiTec (Göttingen, Germany).

For nuclear staining, 4',6'-diamidino-2-phenylindole (Boehringer Mannheim, Mannheim, Germany) was used.

For real-time PCR TaqMan[®] MGB probes, FAM[™] dye-labeled for occludin (Hs00170162_m1), ZO-1 (Hs00268480_m1), Cldn-4 (Hs00430426_m1), and 18S RNA (Hs99999901_s1) were purchased from Applied Biosystems (Foster City, CA).

HaCaT cell and pig organ skin cultures

The cultivation of HaCaT cells was performed as described before, using DMEM including 10% fetal calf serum (Moll *et al.*, 1998).

Pig skin was obtained from an intact porcine carcass immediately after death. Ears were removed after slaughtering and delivered by courier to the laboratory. Directly after reception, cleaning, and disinfection of the pig ears (approximately 1 hour after killing), 6-mm punch biopsies were taken and dermis was placed down on sterile gauze in culture dishes and immersed in medium such that the dermis was solely in contact with the medium, while the epidermis remained exposed to air ("air-liquid interphase"). The medium consisted of DMEM supplemented with hydrocortisone, 5% fetal calf serum, penicillin and streptomycin. The resultant *ex-vivo* organ culture model was incubated in ambient air with 10% CO₂ at 37°C for up to 5 days.

Cultivation of bacteria

Bacteria were grown for 6 hours in Trypticase-soy-broth to end-exponential phase and 100 μ l were spread onto Columbia blood agar plates and incubated at 38°C overnight without antibiotics, resulting in bacteria in post-exponential growth phase. For preparation of suspensions containing defined bacterial cell counts, the respective strains were suspended in HaCaT medium to an OD₆₀₀ between 10¹⁰–10¹¹ CFU/ml. Using this suspension, bacteria were diluted in HaCaT medium to final densities of 10⁵, 10⁶, and 10⁷ CFU/ml.

Infection of HaCaT cell cultures and pig infection model

HaCaT cells were grown in culture dishes and on coverslips until confluency and subsequently infected with bacteria of the strains *S. epidermidis* and *S. aureus* in various concentrations (10 ml of 10⁴–10⁶ bacteria per ml; 3 \times 10⁶ keratinocytes per plate, resulting in bacteria:keratinocyte ratios of 1:30, 1:3, and 3:1, respectively).

Porcine ear skin punch biopsies were cultured as the above described *ex vivo* cultivation model. After 24 hours pre-incubation at 37°C and 10% CO₂, biopsies were infected with smears of the different *Staphylococcus* strains in the post-exponential phase for another 6, 12, and 24 hours.

Immunofluorescence microscopy

Cryostat sections (4–7 μ m) of porcine frozen tissue were fixed in acetone at –20°C for 10 minutes. Cultured cells were fixed in cold methanol (–20°C, 5 minutes) and acetone (–20°C, 30 seconds). Paraffin sections of human skin were deparaffinated and rehydrated. Staining was essentially performed as described previously (Brandner *et al.*, 2002). Briefly, primary antibodies were diluted in phosphate-buffered saline (Cldn-1: 1:150 (cells), 1:300 (tissues); Cldn-4: 1:150 (cells); occludin: 1:100 (cells and tissues); ZO-1: 1:200 (cells), 1:300 (tissues); aPKC: 1:100 (cells); E-Cadherin: 1:5 (cells), 1:100 (tissues); β -Catenin 1:200 (cells), 1:50 (tissues); desmoplakin I+II 1:60 (cells and tissues); Ki67 1:50 (tissues); Protein A 1:500 (tissues)) and applied to the sections for 30 minutes at room temperature. For some of the antibodies (occludin, ZO-1, desmoplakin I+II) a blocking step (2% NGS, 0.1% Triton X-100; 15 minutes room temperature) preceded the antibody-incubation. The samples were subsequently washed for 3 \times 10 minutes. Afterwards, Alexa 488- and Alexa 594-coupled secondary antibodies were applied for 30 minutes at room temperature, followed by another washing and a subsequent incubation with 4',6'-diamidino-2-phenylindole (1:5,000 in phosphate-buffered saline). Finally the slides or coverslips were again washed with phosphate-buffered saline, followed by aqua dest and mounted with Fluoromount (Southern Biotechnology Associates Inc. Birmingham, AL). Isotype-matched antibodies were used for negative controls. An Axiophot II microscope (Zeiss, Göttingen, Germany) and the software Openlab 2.0.4 (Improvision, Coventry, UK) were used for the evaluation of stainings. All images of stainings from a series of experiments were acquired and processed with the same settings and representative areas were scanned.

TER experiment

HaCaT cells were trypsinized and plated onto Transwell Permeable Supports with 12 mm diameter inserts and a pore size of 0.4 μ m (Corning Incorporated, Corning, NY), with a cell density of 50,000 cells/well. When cells reached confluence they were transferred to differentiation medium (Uchida *et al.*, 2001). *S. aureus* and *S. epidermidis* respectively (diluted in cell culture medium) were applied to the upper chamber of the Transwell inserts onto the HaCaT cell layers (0 hour). Subsequently repeated, sequential TER measurements of the individual monolayers were performed with a Millicell-ERS epithelial voltohmmeter (Millipore, Schwalbach, Germany) at 0, 3, 4, 5, 7.5, 9, and 10 hours, with electrodes, reproducibly placed. TER values were calculated by subtracting the contribution of the bare filter and medium. There was no continuity between the fluid from the upper chamber and the lower chamber of the Transwells, and no growth of bacteria was seen in the lower chamber at early time points of the experiment. However, it cannot be totally excluded that secreted material of *S. aureus* can reach the lower chamber independent of the condition of HaCaT cells.

Apoptosis assay

For evaluation of apoptotic cells within porcine skin, we used an established, commercially available TUNEL kit (Apop Tag, INTERGEN, Purchase, NY) with anti-digoxigenin FITC-conjugated antibodies. Negative controls were performed by omitting TdT; human spleen served as positive controls. For more detailed description, see previous publications (Foitzik *et al.*, 2000). To evaluate differences

between the infection and control group, statistical analysis was performed by using Wilcoxon test.

Evaluation of stainings

Immunoreactivity of the stainings of the various cell-cell junction proteins on skin infection models with and without infection were classified into "normal staining", that is, as found in normal (porcine) skin, "enhanced staining", that is, more widespread (vertically or horizontally) than in normal skin, "reduced staining", that is, less intensive than in normal skin, and "loss of staining", that is, no staining was visible. Two sections per staining and model were evaluated. All sections showed areas with normal staining in addition to enhanced, reduced, or loss of staining, which were used as internal controls. In models exhibiting normal and altered staining only altered staining was considered for analysis.

Models evaluated (per bacterial strain/control) 6 hours, Cldn-1 ≥ 4 , Occl ≥ 5 , ZO-1 ≥ 5 , E-Cad ≥ 3 , β -Cat ≥ 4 , Dp I+II ≥ 4 ; 12 hours, Cldn-1 ≥ 4 , Occl ≥ 4 , ZO-1 ≥ 4 , E-Ca ≥ 3 , β -Cat ≥ 3 , Dp I+II ≥ 3 ; 24 hours, Cldn-1 ≥ 4 , Occl ≥ 4 , ZO-1 ≥ 4 , E-Cad ≥ 3 , β -Cat ≥ 4 , Dp I+II ≥ 3 .

Total count of evaluated models were as follows: 6 hours, $n=32$; 12 hours, $n=22$ and 24 hours, $n=60$. In ambiguous test serious, up to 15 models were evaluated (eg, 24-hour control).

Isolation of RNA, reverse transcription, and real-time PCR

Total mRNA was isolated by using the RNeasy mini kit (Qiagen, Hilden, Germany) according to the manufacturer's instructions. A 3 μ g weight of total RNA was utilized for first-strand cDNA synthesis with the iScript cDNA synthesis kit (BioRad, Munich, Germany), as suggested by the manufacturer. A 2 μ l volume of the cDNA reaction was used as a template in real-time PCR analysis with FAMTM dye-labeled real-time PCR TaqMan[®] MGB probes for Cldn-4, occludin, and ZO-1 in an iCycler iQ thermal cycler under the conditions recommended by Applied Biosystems. All reverse transcription-PCR analyses were performed in triplicate for five (3-hour values) and three (5-hour values) independent experiments. Relative transcriptional levels within distinct experiments were determined by the $2^{-\Delta\Delta C_t}$ method (Livak and Schmittgen, 2001). Statistical analysis were performed with Student's *t*-test.

Bacterial DNA preparation and detection of virulence-associated genes

DNA was prepared essentially as described previously (Rohde et al., 2005). For the detection of genes encoding factors involved in adhesion to extracellular matrix components (*fnbA*, *clfA*, *cna*, *bbp*, *map/eap*, *spa*, *sdtD*, *sasG*), PCR was carried out using primers and conditions as described (Peacock et al., 2002).

Western blot analysis

HaCAT cells were washed with phosphate-buffered saline and subsequently lysed in radioimmunoprecipitation assay buffer containing 1% NP-40, 0.5% deoxycholate, 0.1% SDS, 5 mM EDTA, 150 mM NaCl, 50 mM Tris, pH 8.0, and a cocktail of protease inhibitors (Sigma). Equal amounts of total protein (15 μ g) were separated by SDS-PAGE and transferred to nitrocellulose. After blocking for 1 hours with 5% dry milk powder in tris buffered saline + triton (TBST), membranes were probed with the appropriate antibodies (Cldn-1: 1:400; Cldn-4: 1:100; Cldn-7: 1:200; occludin:

1:100; JAM-A: 1:200; ZO-1: 1:150; aPKC: 1:200; E-Cadherin: 1:100; β -Catenin: 1:150; α -Tubulin: 1:150 in TBST) overnight at 4°C. Subsequently membranes were washed 3 \times 5 minutes with TBST and incubated for 30 minutes with the appropriate secondary antibodies coupled with horseradish peroxidase. After another washing 2 \times 5 minutes with TBST immunoreactions were visualized by enhanced chemiluminescence.

CONFLICT OF INTEREST

The authors state no conflict of interest.

ACKNOWLEDGMENTS

We thank Dr Gefion Franke for stimulating discussions and technical support. This work was supported by the Hooke-Stiftung.

SUPPLEMENTARY MATERIAL

Table S1. Bacterial strains used in this study and distribution of genes encoding cell-surface proteins involved in adhesion to extracellular matrix molecules and exotoxins.

Figure S1. Comparison of the localization of the TJ-associated proteins ZO-1 and aPKC, and the AJ protein E-Cadherin 5 hours after infection with *S. aureus* and *S. epidermidis*.

Figure S2. Immunoreactivity of TJ, AJ, and desmosomal proteins in porcine skin infection models 6 and 12 hours following infection with *S. aureus* ATCC 29213, clinical isolate, and *S. epidermidis* 1457.

Figure S3. Expression of TJ, AJ, and desmosomal proteins in porcine skin infection models 24 hours following infection with *S. aureus* ATCC 29213, clinical isolate, RN 6390, and Newman.

REFERENCES

- Amagai M, Matsuyoshi N, Wang ZH, Andl C, Stanley JR (2000) Toxin in bullous impetigo and staphylococcal scalded-skin syndrome targets desmoglein 1. *Nat Med* 6:1275-7
- Amagai M, Yamaguchi T, Hanakawa Y, Nishifuji K, Sugai M, Stanley JR (2002) Staphylococcal exfoliative toxin B specifically cleaves desmoglein 1. *J Invest Dermatol* 118:845-50
- Boukamp P, Petrussevska RT, Breitkreutz D, Hornung J, Markham A, Fusenig NE (1988) Normal keratinization in a spontaneously immortalized aneuploid human keratinocyte cell line. *J Cell Biol* 106:761-71
- Brandner JM, Kief S, Grund C, Rendl M, Houdek P, Kuhn C et al. (2002) Organization and formation of the tight junction system in human epidermis and cultured keratinocytes. *Eur J Cell Biol* 81:253-63
- Brandner JM, Kief S, Wladykowski E, Houdek P, Moll I (2006) Tight junction proteins in the skin. *Skin Pharmacol Physiol* 19:71-7
- Breuer K, Wittmann M, Kempe K, Kapp A, Mai U, Dittrich-Breiholz O et al. (2005) Alpha-toxin is produced by skin colonizing *Staphylococcus aureus* and induces a T helper type 1 response in atopic dermatitis. *Clin Exp Allergy* 35:1088-95
- Cywes C, Wessels MR (2001) Group A *Streptococcus* tissue invasion by CD44-mediated cell signalling. *Nature* 414:648-52
- Fasano A (2001) Intestinal zonulin: open sesame!. *Gut* 49:159-62
- Fasano A (2002) Toxins and the gut: role in human disease. *Gut* 50(Suppl 3):III9-14
- Foitzik K, Lindner G, Mueller-Roever S, Maurer M, Botchkareva N, Botchkarev V et al. (2000) Control of murine hair follicle regression (catagen) by TGF-beta1 *in vivo*. *FASEB J* 14:752-60
- Fudaba Y, Nishifuji K, Andresen LO, Yamaguchi T, Komatsuzawa H, Amagai M et al. (2005) *Staphylococcus hyicus* exfoliative toxins selectively digest porcine desmoglein 1. *Microb Pathog* 39:171-6
- Furuse M, Hata M, Furuse K, Yoshida Y, Haratake A, Sugitani Y et al. (2002) Claudin-based tight junctions are crucial for the mammalian epidermal barrier: a lesson from claudin-1-deficient mice. *J Cell Biol* 156:1099-111

- Furuse M, Tsukita S (2006) Claudins in occluding junctions of humans and flies. *Trends Cell Biol* 16:181–8
- Iwatsuki K, Yamasaki O, Morizane S, Oono T (2006) Staphylococcal cutaneous infections: invasion, evasion and aggression. *J Dermatol Sci* 42:203–14
- Langbein L, Grund C, Kuhn C, Praetzel S, Kartenbeck J, Brandner JM *et al.* (2002) Tight junctions and compositionally related junctional structures in mammalian stratified epithelia and cell cultures derived therefrom. *Eur J Cell Biol* 81:419–35
- Laukoetter MG, Bruewer M, Nusrat A (2006) Regulation of the intestinal epithelial barrier by the apical junctional complex. *Curr Opin Gastroenterol* 22:85–9
- Leung D, Hauk P, Strickland I, Travers J, Norris D (1998) The role of superantigens in human diseases: therapeutic implications for the treatment of skin diseases. *Br J Dermatol* 139:17–29
- Lewis JE, Jensen PJ, Johnson KR, Wheelock MJ (1994) E-cadherin mediates adherens junction organization through protein kinase C. *J Cell Sci* 107(Part 12):3615–21
- Leyvraz C, Charles RP, Rubera I, Guitard M, Rotman S, Breiden B *et al.* (2005) The epidermal barrier function is dependent on the serine protease CAP1/Prss8. *J Cell Biol* 170:487–96
- Livak KJ, Schmittgen TD (2001) Analysis of relative gene expression data using real-time quantitative PCR and the 2(–Delta Delta C(T)) Method. *Methods* 25:402–8
- Matter K, Balda MS (2003a) Functional analysis of tight junctions. *Methods* 30:228–34
- Matter K, Balda MS (2003b) Signalling to and from tight junctions. *Nat Rev Mol Cell Biol* 4:225–36
- Mertens AE, Pegtel DM, Collard JG (2006) Tiam1 takes PART in cell polarity. *Trends Cell Biol* 16:308–16
- Moll I, Houdek P, Schmidt H, Moll R (1998) Characterization of epidermal wound healing in a human skin organ culture model: acceleration by transplanted keratinocytes. *J Invest Dermatol* 111:251–8
- Murakawa GJ (2004) Common pathogens and differential diagnosis of skin and soft tissue infections. *Cutis* 73:7–10
- Muza-Moons MM, Schneeberger EE, Hecht GA (2004) Enteropathogenic *Escherichia coli* infection leads to appearance of aberrant tight junctions strands in the lateral membrane of intestinal epithelial cells. *Cell Microbiol* 6:783–93
- Peacock SJ, Moore CE, Justice A, Kantzanou M, Story L, Mackie K *et al.* (2002) Virulent combinations of adhesin and toxin genes in natural populations of *Staphylococcus aureus*. *Infect Immun* 70:4987–96
- Pummi K, Malminen M, Aho H, Karvonen S-L, Peltonen J, Peltonen S (2001) Epidermal tight junctions: ZO-1 and occludin are expressed in mature, developing, and affected skin and *in vitro* differentiating keratinocytes. *J Invest Dermatol* 117:1050–8
- Rohde H, Burdelski C, Bartscht K, Hussain M, Buck F, Horstkotte MA *et al.* (2005) Induction of *Staphylococcus epidermidis* biofilm formation via proteolytic processing of the accumulation-associated protein by staphylococcal and host proteases. *Mol Microbiol* 55:1883–95
- Schneeberger EE, Lynch RD (2004) The tight junction: a multifunctional complex. *Am J Physiol Cell Physiol* 286:C1213–28
- Sonoda N, Furuse M, Sasaki H, Yonemura S, Katahira J, Horiguchi Y *et al.* (1999) *Clostridium perfringens* enterotoxin fragment removes specific claudins from tight junction strands: evidence for direct involvement of claudins in tight junction barrier. *J Cell Biol* 147:195–204
- Travers J, Norris D, Leung Y (2001) The keratinocyte as a target for staphylococcal bacterial toxins. *J Invest Dermatol Symp Proc* 6:225–30
- Tsukita S, Furuse M (2002) Claudin-based barrier in simple and stratified cellular sheets. *Curr Opin Cell Biol* 14:531–6
- Tunggal JA, Helfrich I, Schmitz A, Schwarz H, Gunzel D, Fromm M *et al.* (2005) E-cadherin is essential for *in vivo* epidermal barrier function by regulating tight junctions. *EMBO J* 24:1146–56
- Turksen K, Troy TC (2002) Permeability barrier dysfunction in transgenic mice overexpressing claudin 6. *Development* 129:1775–84
- Uchida Y, Behne M, Quiec D, Elias PM, Holleran WM (2001) Vitamin C stimulates sphingolipid production and markers of barrier formation in submerged human keratinocyte cultures. *J Invest Dermatol* 117:1307–13
- Vasioukhin V, Bauer C, Yin M, Fuchs E (2000) Directed actin polymerization is the driving force for epithelial cell–cell adhesion. *Cell* 100:209–19
- Yoshida Y, Morita K, Mizoguchi A, Ide C, Miyachi Y (2001) Altered expression of occludin and tight junction formation in psoriasis. *Arch Dermatol Res* 293:239–44